

Technical Notes

TECHNICAL NOTES are short manuscripts describing new developments or important results of a preliminary nature. These Notes cannot exceed six manuscript pages and three figures; a page of text may be substituted for a figure and vice versa. After informal review by the editors, they may be published within a few months of the date of receipt. Style requirements are the same as for regular contributions (see inside back cover).

Resolving the Dependence on Freestream Values for the k - ω Turbulence Model

Johan C. Kok*

National Aerospace Laboratory NLR,
1006 BM Amsterdam, The Netherlands

I. Introduction

THE k - ω two-equation eddy-viscosity model has become a widely used turbulence model for wall-bounded, aerodynamic flows for two main reasons: it does not require any wall-damping functions or the computation of wall distances, and it is less stiff than k - ϵ models in the near-wall region. In particular, the first property is desirable for complex configurations. However, the original k - ω model of Wilcox^{1,2} has one main drawback: the results depend on the freestream value of the turbulence variables (in particular ω) even at very low freestream eddy-viscosity levels. This freestream dependence seems to be the strongest for free shear layers but is also significant for boundary layers. As shown by Menter,³ a correct solution for boundary layers can be obtained if a sufficiently large value of ω is applied at the boundary-layer edge. In practice, however, it is difficult to obtain such a large value at the boundary-layer edge because the turbulence variables are generally prescribed at a far-field boundary and will decay in the freestream.

Because the k - ϵ model generally does not seem to have this freestream dependency, Menter⁴ proposed to resolve the freestream dependency by a blending between the standard Wilcox model and the standard k - ϵ model (in a k - ω formulation). The model switches from k - ω to k - ϵ approaching the boundary-layer edge, with as main effect the inclusion of an extra term (the so-called cross-diffusion term) in the ω equation. However, the wall distance is required to evaluate the blending function, thus losing one of the advantages of the k - ω model. Wilcox⁵ proposed to include the cross-diffusion term without any blending functions and to switch it off when it becomes negative so that it is not effective in the near-wall region, which is crucial for a correct behavior of the k - ω model. The analysis and results in this Note, however, will show that with the model coefficients chosen by Wilcox this model does not effectively resolve the freestream dependency.

An alternative approach is to enforce the correct (large) value of ω at the boundary-layer edge. See, for example, the k - g model of Kalitzin et al.⁶ or the background production as suggested by de Cock.⁷ A second alternative is to redesign the model such that a correct solution is obtained for a sufficiently small (instead of sufficiently large) freestream value of ω , as done recently by Wilcox.²

The behavior of the k - ϵ type models at freestream edges of turbulent regions was studied by Cazalbou et al.⁸ A one-dimensional model problem was considered together with a particular, weak solution representing a front between a turbulent and a nonturbulent region. Constraints were derived for which the weak solution is valid

and for which the front moves into the nonturbulent region. It was demonstrated that most k - ϵ models show the weak solution, also in practical situations, and that for such weak solutions the freestream dependency is weak.

In this Note the analysis of Cazalbou et al.⁸ is extended to the k - ω model including the cross-diffusion term. A new set of diffusion coefficients is derived that effectively resolves the freestream dependency, as demonstrated by computations for the flat plate and the RAE2822 airfoil. All computations have been performed with the NLR flow-simulation system ENFLOW for multiblock structured grids.⁹

II. Analysis

The k - ω model equations, including the cross-diffusion term, are given by

$$\frac{\partial \rho k}{\partial t} + \frac{\partial (\rho k u_j)}{\partial x_j} = P_k - \beta^* \rho \omega k + \frac{\partial}{\partial x_j} \left((\mu + \sigma_k \mu_t) \frac{\partial k}{\partial x_j} \right) \quad (1)$$

$$\frac{\partial \rho \omega}{\partial t} + \frac{\partial (\rho \omega u_j)}{\partial x_j} = P_\omega - \beta \rho \omega^2 + \frac{\partial}{\partial x_j} \left((\mu + \sigma_\omega \mu_t) \frac{\partial \omega}{\partial x_j} \right) + C_D \quad (2)$$

with ρ the density, \mathbf{u} the velocity vector, μ the molecular-viscosity coefficient, k the turbulent kinetic energy, ω the specific turbulent dissipation, and $\mu_t = \rho k / \omega$ the eddy-viscosity coefficient. The production terms are $P_k = \tau_{ij}^R \partial u_i / \partial x_j$ and $P_\omega = \alpha_\omega \omega P_k / k$, with τ^R the Reynolds-stress tensor, and the cross-diffusion term is given by

$$C_D = \sigma_d \frac{\rho}{\omega} \max \left\{ \frac{\partial k}{\partial x_i} \frac{\partial \omega}{\partial x_i}, 0 \right\} \quad (3)$$

The k - ω model has six closure coefficients: α_ω , β^* , β , σ_k , σ_ω , and σ_d . Following Wilcox,¹ four relations between these coefficients can be derived. First, to be consistent with the experimental decay of the turbulent kinetic energy for homogeneous, isotropic turbulence, $\beta^* / \beta = \frac{6}{5}$. Second, to obtain the correct solution in the inner layer of a constant-pressure boundary layer, consistent with the law of the wall, $\alpha_\omega = \beta / \beta^* - \sigma_\omega \kappa^2 / \sqrt{\beta^*}$ (with $\kappa = 0.41$ the von Kármán constant), and $\beta^* = 0.09$, while further $\sigma_\omega = 0.5$ or otherwise a low-Reynolds-number modification is needed.⁵ The effect of the two remaining coefficients, σ_k and σ_d , on the solution in the inner layer is weak; they will be tuned to obtain a desirable behavior of the model at the boundary-layer edge.

Following Cazalbou et al.,⁸ the following set of one-dimensional diffusion equations is considered as a model for freestream edges of turbulent regions:

$$\frac{\partial k}{\partial t} = \frac{\partial}{\partial y} \left(\sigma_k v_t \frac{\partial k}{\partial y} \right) \quad (4)$$

$$\frac{\partial \omega}{\partial t} = \frac{\partial}{\partial y} \left(\sigma_\omega v_t \frac{\partial \omega}{\partial y} \right) + \sigma_d \frac{1}{\omega} \frac{\partial k}{\partial y} \frac{\partial \omega}{\partial y} \quad (5)$$

$$\frac{\partial u}{\partial t} = \frac{\partial}{\partial y} \left(v_t \frac{\partial u}{\partial y} \right) \quad (6)$$

with $v_t = k / \omega$ and with the diffusion coefficients σ_k , $\sigma_\omega > 0$, and $\sigma_d \geq 0$. This set of equations has a particular weak solution,

Received 21 September 1999; revision received 7 March 2000; accepted for publication 7 March 2000. Copyright © 2000 by Johan C. Kok. Published by the American Institute of Aeronautics and Astronautics, Inc., with permission.

*Research Scientist, P.O. Box 90502; jkok@nlr.nl.

consisting of a front between a turbulent and a nonturbulent region moving with a velocity c in the positive y direction:

$$\begin{aligned} k &= k_0 f^{\sigma_\omega / (\sigma_\omega - \sigma_k + \sigma_d)}, & \omega &= \omega_0 f^{(\sigma_k - \sigma_d) / (\sigma_\omega - \sigma_k + \sigma_d)} \\ u &= u_0 f^{\sigma_k \sigma_\omega / (\sigma_\omega - \sigma_k + \sigma_d)}, & v_t &= (k_0 / \omega_0) f \end{aligned} \quad (7)$$

with

$$f = \max \left\{ \frac{ct - y}{\delta_0}, 0 \right\}, \quad c = \frac{k_0}{\omega_0 \delta_0} \frac{\sigma_k \sigma_\omega}{\sigma_\omega - \sigma_k + \sigma_d} \quad (8)$$

and with k_0 , ω_0 , and δ_0 positive constants. (For $y > ct$, $\omega = 0$ is not a strict solution of the equations; in practice, small nonzero values for k and ω are used in the freestream.)

A number of constraints can be derived from this particular solution. First, for this solution to be a valid weak solution of the model problem, the three transported variables (k , ω , and u) must go to

zero when approaching the front from the side $y < ct$, resulting in the constraints

$$\sigma_\omega - \sigma_k + \sigma_d > 0 \quad (9)$$

$$\sigma_k - \sigma_d > 0 \quad (10)$$

Second, the slope of u at the front is required to be finite (physically valid), resulting in

$$\sigma_\omega - \sigma_k + \sigma_d \leq \sigma_k \sigma_\omega \quad (11)$$

Constraint (10) ensures that the slope of k at the front is also finite. Third, for the particular solution of the model problem to be representative for the solution of the k - ω model at a boundary-layer edge, we require the production and dissipation terms in the k and ω equations to be negligible compared to the diffusion terms when approaching the front. For the k equation the diffusion, production,

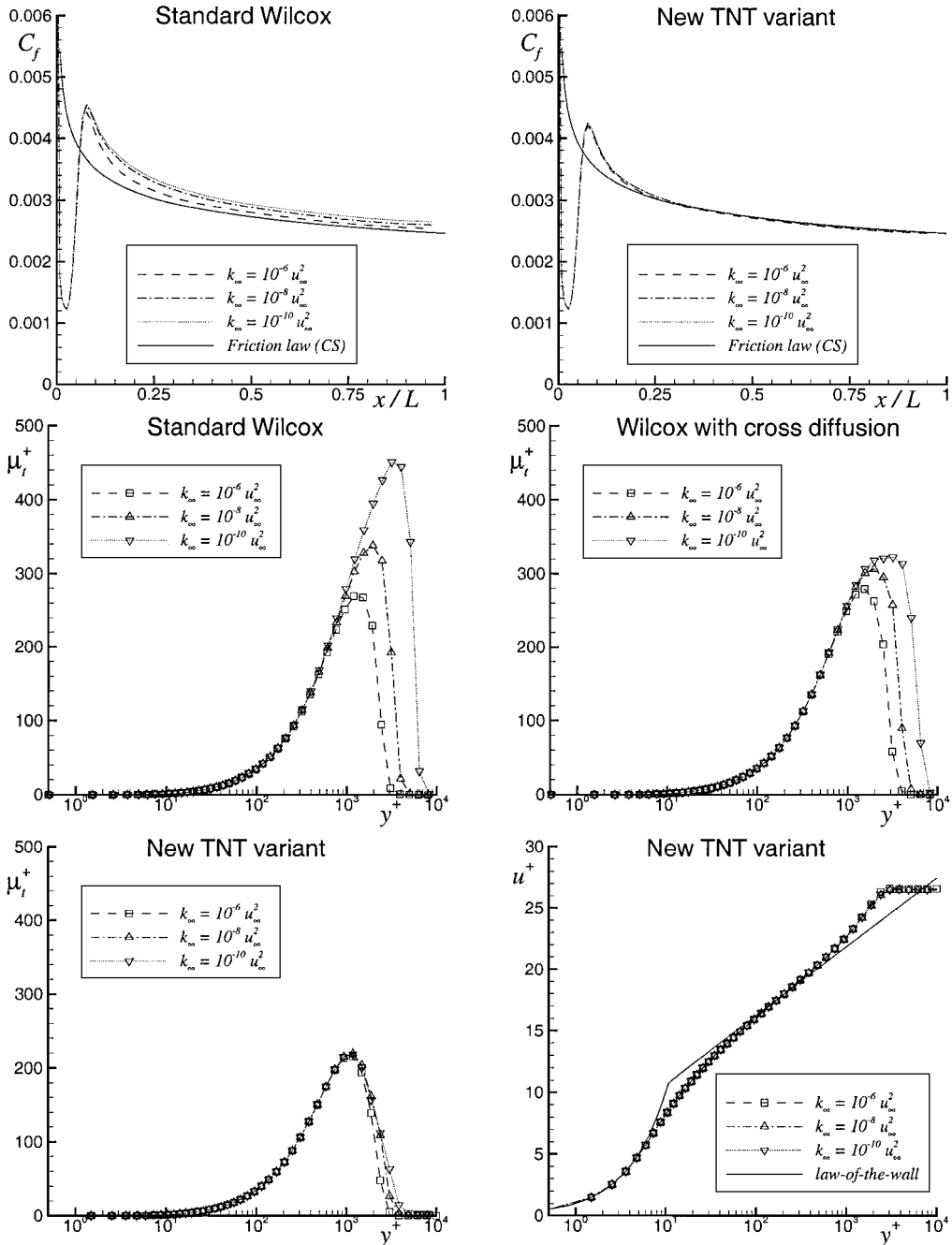


Fig. 1 Solutions of various k - ω models for flat plate at $Re_\infty = 10^7$, $M_\infty = 0.5$, and $Re_{t,\infty} = 10^{-2}$. Eddy-viscosity and velocity distributions (law-of-the-wall scaling) at $x/L = 0.5$. Transition: 5% from leading edge. Grid: 64×64 grid cells, with 40 on the flat plate, 30 to 40 in the boundary layer, and $y^+ \approx 1$ for first grid point.

and dissipation terms are

$$\frac{\partial}{\partial y} \left(\sigma_k v_t \frac{\partial k}{\partial y} \right) \sim f^{(\sigma_k - \sigma_d)/(\sigma_\omega - \sigma_k + \sigma_d)} \quad (12)$$

$$v_t \left(\frac{\partial u}{\partial y} \right)^2 \sim f^{[(2\sigma_k - 1)\sigma_\omega + \sigma_k - \sigma_d]/(\sigma_\omega - \sigma_k + \sigma_d)} \quad (13)$$

$$\beta^* k \omega \sim f^{(\sigma_\omega + \sigma_k - \sigma_d)/(\sigma_\omega - \sigma_k + \sigma_d)} \quad (14)$$

Requiring the power of f in the production and dissipation terms to be larger than the power of f in the diffusion term, one obtains the constraints

$$\sigma_k > 0.5, \quad \sigma_\omega > 0 \quad (15)$$

For the ω equation the same constraints are obtained.

An important consequence of constraint (9) is that the velocity of the front is positive ($c > 0$). Thus, the front moves into the non-turbulent region. On this basis, one can expect the dependence of the solution on the freestream values of k and ω to be weak (if the freestream eddy viscosity is negligibly small).

The standard Wilcox model ($\sigma_\omega = 0.5$, $\sigma_k = 0.5$, $\sigma_d = 0$) as well as the Wilcox model including cross diffusion ($\sigma_\omega = 0.6$, $\sigma_k = 1.0$, $\sigma_d = 0.3$) do not satisfy constraint (9). For the Menter baseline model the set of coefficients obtained near the boundary-layer edge ($\sigma_\omega = 0.856$, $\sigma_k = 1.0$, $\sigma_d = 2\sigma_\omega$) satisfies constraint (9), resulting in a positive velocity of the front, but not constraint (10), so that the weak solution is not strictly valid (ω goes to infinity when approaching the front).

The following new choice of values for the diffusion coefficients, denoted as the turbulent/nonturbulent (TNT) set,

$$\sigma_\omega = 0.5, \quad \sigma_k = \frac{2}{3}, \quad \sigma_d = 0.5 \quad (16)$$

satisfies all formulated constraints of the TNT analysis just shown. Note that $\sigma_\omega = 0.5$ so that low-Reynolds modifications are not needed.

III. Results

As a first test case, the flat-plate constant-pressure boundary layer is considered at a Reynolds number of $Re_\infty = 10^7$ and a free-stream turbulent Reynolds number of $Re_{t,\infty} = (\mu_t/\mu)_\infty = 10^{-2}$. The freestream value of k is varied by several orders of magnitude, thus also varying the freestream value of ω . Figure 1 shows the computed skin-friction coefficients, compared to the skin-friction law given by Cebeci and Smith¹⁰ [Eq. (5.4.23)], as well as the velocity and eddy-viscosity distributions at the location $Re_x = 5 \times 10^6$.

For the standard Wilcox model as well as for the Wilcox model with cross diffusion, the dependency of the solution on the freestream values is apparent. This dependency is most clearly revealed for the eddy-viscosity distribution. The transport of low freestream values of ω into the boundary layer results in a net production of eddy viscosity near the boundary-layer edge, which becomes stronger as the freestream value of ω is decreased. The larger eddy-viscosity levels cause an increase of the skin-friction coefficient. To obtain the correct solution, the value of ω at the boundary-layer edge should be sufficiently large as pointed out by Menter.³ In practice, this value is not obtained (even for the largest value of k_∞) because the value of ω has decayed before the boundary-layer edge is reached. As a consequence, the skin-friction distribution lies above the theoretical law.

Consistent with the analysis, the computations with the TNT choice of diffusion coefficients show practically no freestream dependency. Although the distribution of the eddy viscosity at the

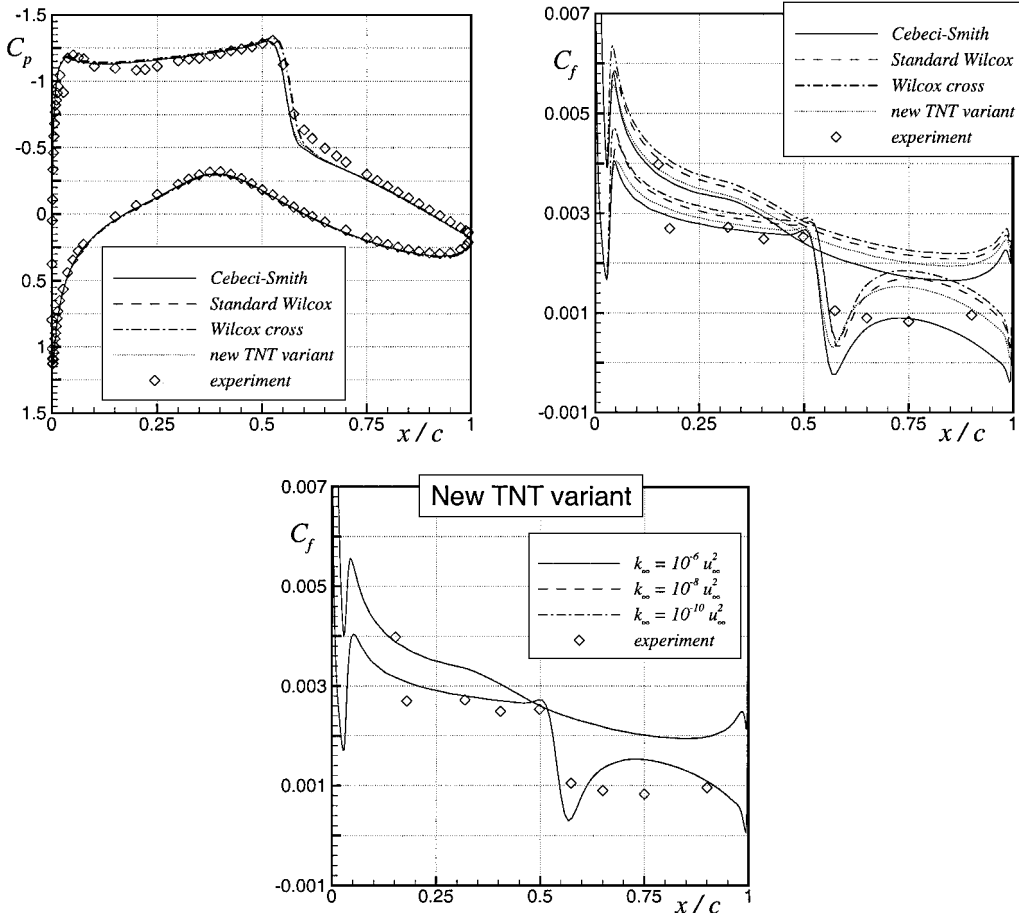


Fig. 2 Solution of various k - ω models and Cebeci-Smith model for RAE2822 airfoil, case 9 ($M_\infty = 0.73$, $Re_\infty = 6.5 \times 10^6$, $\alpha = 2.8^\circ$, $Re_{t,\infty} = 10^{-2}$, $k_\infty = 10^{-6} u_\infty^2$). Transition: 3% from leading edge. Grid: 528×96 grid cells with 384 around the airfoil, 30 to 40 in the boundary layer, $y^+ < 1$ for first grid point, and far field at 50 chords.

boundary-layer edge is still slightly freestream dependent, the level of eddy viscosity and therefore also the skin-friction coefficient are not. Furthermore, the velocity distribution is consistent with the law-of-the-wall solution.

As a second test case, the RAE2822 airfoil is considered (in particular, case 9 of Ref. 11). Figure 2 compares the pressure and skin-friction distributions of the different models to the experimental results. For the two Wilcox variants the shock is located slightly aft compared to the Cebeci-Smith model and the new $k-\omega$ variant. Similarly as for the flat plate, the TNT $k-\omega$ variant gives lower levels of the skin friction than the two Wilcox variants, and in this case closer to the Cebeci-Smith model and to the experimental values. Most likely, the more aft shock position and the higher skin friction for the two Wilcox variants are a result of higher eddy-viscosity levels (as were seen for the flat plate). This again may be a consequence of the values of ω at the boundary-layer edge being too low. For the TNT $k-\omega$ variant the absence of freestream dependency is shown for the skin-friction coefficient.

IV. Conclusions

The theoretical analysis of TNT interfaces presented in this Note has resulted in a set of constraints that the diffusion coefficients of the $k-\omega$ model (including the cross-diffusion term) should satisfy to resolve the freestream dependency for a model problem. A new set of diffusion coefficients has been chosen that satisfies this set of constraints. Furthermore, these TNT coefficients allow the correct near-wall solution for a constant-pressure boundary layer without the introduction of any blending functions or near-wall modifications, i.e., without introducing the wall distance. Computations for a flat-plate constant-pressure boundary layer and for a two-dimensional airfoil have demonstrated the effective elimination of the freestream dependency at low freestream eddy-viscosity levels, while maintaining the correct near-wall solution.

Acknowledgments

The ENFLOW system has been developed under Contract 01105N awarded by the Netherlands Agency for Aerospace Programmes. To some extent the analysis presented here has been carried out within the framework of the Advanced Viscous Flow Simulation Tools for Complete Civil Transport Aircraft Design (AVTAC) project. The AVTAC project is a collaboration of BAE SYSTEMS, Daimler-Benz Aerospace, Construcciones Aeronauticas SA, Dassault Aviation, Saab, Alenia, German Aerospace Research Center DLR, ONERA, Italian Aerospace Research Center, FFA, and National Aerospace Laboratory NLR. The project is managed by BAE SYSTEMS and is funded by the Commission of European Communities under the Industrial and Materials Technologies initiative (Project BRPR CT97-0555). The author wishes to thank B. Oskam and K. M. J. de Cock for reviewing the manuscript.

References

- ¹Wilcox, D. C., "Reassessment of the Scale-Determining Equation for Advanced Turbulence Models," *AIAA Journal*, Vol. 26, No. 11, 1988, pp. 1299-1310.
- ²Wilcox, D. C., *Turbulence Modeling for CFD*, 2nd ed., DCW Industries, Inc., La Cañada, CA, 1998, pp. 119-122.
- ³Menter, F. R., "Influence of Freestream Values on $k-\omega$ Turbulence Model Predictions," *AIAA Journal*, Vol. 30, No. 16, 1991, pp. 1657-1659.
- ⁴Menter, F. R., "Zonal Two Equation $k-\omega$ Turbulence Models for Aerodynamic Flows," AIAA Paper 93-2906, July 1993.
- ⁵Wilcox, D. C., "A Two-Equation Turbulence Model for Wall-Bounded and Free-Shear Flows," AIAA Paper 93-2905, July 1993.
- ⁶Kalitzin, G., Gould, A. R. B., and Benton, J. J., "Application of Two-Equation Turbulence Models in Aircraft Design," AIAA Paper 96-0327, Jan. 1996.
- ⁷de Cock, K. M. J., "Fully Automatic Navier-Stokes Algorithm for 2D High-Lift Flows," *Fifteenth International Conference on Numerical Methods in Fluid Dynamics*, Vol. 490, Lecture Notes in Physics, Springer-Verlag, Berlin, 1977, pp. 225-231.
- ⁸Cazalbou, J. B., Spalart, P. R., and Bradshaw, P., "On the Behaviour of Two-Equation Models at the Edge of a Turbulent Region," *Physics of Fluids*, Vol. 6, No. 5, 1994, pp. 1797-1804.
- ⁹Boerstoeel, J. W., Kassies, A., Kok, J. C., and Spekrijse, S. P., "ENFLOW, a Full-Functionality System of CFD Codes for Industrial Euler/Navier-Stokes Flow Computations," National Aerospace Lab. NLR, TP 96286, Amsterdam, May 1996.
- ¹⁰Cebeci, T., and Smith, A. M. O., *Analysis of Turbulent Boundary Layers*, Academic, New York, 1974, pp. 187-191.
- ¹¹Cook, P., McDonald, M., and Firmin, M., "Airfoil RAE 2822—Pressure Distributions and Boundary Layer Wake Measurements," AR 138, AGARD, May 1979.

R. M. C. So
Associate Editor

Numerical Simulation of Unsteady Low-Reynolds-Number Separated Flows over Airfoils

Mahidhar Tatineni* and Xiaolin Zhong†
University of California, Los Angeles,
Los Angeles, California 90095-1597

Introduction

LOW-REYNOLDS-NUMBER aerodynamics, in the range of $Re = 5 \times 10^4 - 1 \times 10^6$, is important for a variety of aircraft, ranging from sailplanes and human-powered aircraft to high-altitude unmanned aerial vehicles.^{1,2} There has been considerable research, both experimental³⁻⁵ and computational,⁶⁻⁸ on low-Reynolds-number flows over airfoils.

The flowfield in low-Reynolds-number flows over airfoils is characterized by the presence of separation bubbles, which have a strong influence on the performance of the airfoils. The experimental investigations have also considered the unsteady features of low-Reynolds-number flows over airfoils. Leblanc et al.³ showed that the peak frequencies measured in the velocity spectra for the instability region match the most amplified wave-number and frequency scaling calculated by linear stability theory. The linear evolution of disturbances in the separation bubble was also observed by Dovgal et al.⁴ They also detailed the nonlinear interactions of the disturbances and the path to transition.

Low-Reynolds-number separation bubbles include flows in both the subsonic and transonic Mach-number regimes. Drela and Giles⁶ and Drela⁸ used a viscous-inviscid approach to calculate transonic low-Reynolds-number flows. The simulations used an Euler formulation coupled with an integral boundary-layer formulation, with a transition prediction formulation of e^n type. Their calculations show the strong influence of separation bubbles on the performance of the airfoils. Lin and Pauley⁷ used an unsteady, incompressible Navier-Stokes approach to compute low-Reynolds-number flows. Their results show the unsteady nature of the separation bubble and the associated periodic vortex shedding. The dominant frequency was shown to be in agreement with the most amplified frequency from the linear stability analysis, of a mixing layer corresponding to the separated boundary layer.

The present study considers numerical simulation and analysis of low-Reynolds-number compressible flows over airfoils to understand the physics of the separated flows. A detailed linear stability analysis of the separated flow is performed to explain the unsteady nature of the flow. Numerical results show an unsteady vortex shedding process, which is shown through a linear stability analysis to correspond to the instability of the separated boundary layer. The

Presented as Paper 97-1929 at the AIAA 28th Fluid Dynamics Conference, Snowmass Village, CO, 29 June-2 July 1997; received 12 September 1997; revision received 15 June 1999; accepted for publication 13 March 2000. Copyright © 2000 by the American Institute of Aeronautics and Astronautics, Inc. All rights reserved.

*Graduate Student. Member AIAA.

†Associate Professor, Mechanical and Aerospace Engineering Department, 420 Westwood Plaza, Engineering IV Building. Member AIAA.